AI Engineering
https://www.sciltp.com/journals/aieng

Article

Intelligent Scenario Generation for Weekly and Daily Power System Operations under Typhoon Conditions

Jinxin Wang, Mengyuan Liu *, Nan Yang, Zhenhuan Song, Jin Chen, Yunqi Zhou and Xueling Hong

College of Electrical Engineering and New Energy, China Three Gorges University, Yichang 443002, China
* Correspondence: liumengyuan@ctgu.edu.cn

How To Cite: Wang, J.; Liu, M.; Yang, N.; et al. Intelligent Scenario Generation for Weekly and Daily Power System Operations under Typhoon Conditions. *AI Engineering* **2025**, *1*(1), 4. https://doi.org/10.53941/aieng.2025.100004

Received: 1 June 2025r
Revised: 23 July 2025
Accepted: 7 August 2025
Published: 19 August 2025

Abstract: Typhoons, as a representative form of extreme weather, pose serious threats to power system security by inducing renewable energy volatility and damaging transmission infrastructure. To address these challenges, this study proposes an intelligent scenario generation framework for weekly and daily power system operations under typhoon conditions, aiming to capture the spatiotemporal impacts of typhoon events and support dispatch optimization under extreme weather conditions. The framework first integrates ARIMA-based deterministic forecasting with Monte Carlo simulation to construct stochastic scenario ensembles that capture the variability in renewable generation and load. Then, it applies numerical integration to estimate the probabilities of transmission line faults under the wind stress induced by typhoons. Finally, clustering analysis is used to extract representative and extreme operational scenarios, and a multi-scenario dynamic simulation model is established to evaluate system stability and quantify operational risks. The proposed methodology effectively captures the spatiotemporal characteristics of typhoon impacts on power systems and provides theoretical support for dispatch optimization, fault risk assessment, and resilience enhancement in complex meteorological environments.

Keywords: typhoon-induced uncertainty; scenario generation; ARIMA forecasting; Monte Carlo simulation; line fault probability; cluster analysis

1. Introduction

With the extensive application of renewable energy and the increasing frequency of extreme weather events, modern power systems are facing escalating complex uncertainties [1,2]. Among these extreme weather, typhoons have emerged as a critical threat due to their dual impact: inducing drastic fluctuations in wind power output and causing physical damage to transmission infrastructure [3]. These disturbances significantly amplify the uncertainty of power dispatch and pose serious challenges to the dynamic stability of grid operations. Therefore, it is imperative to develop a scenario generation method that is both accurate and adaptive, capable of comprehensively characterizing the source–load–grid coupled dynamics induced by typhoon processes [4].

Existing studies on scenario generation under extreme weather conditions can be broadly categorized into two methodological paradigms: data-driven learning-based approaches and probabilistic statistical frameworks [5,6]. Deep learning models, including variational autoencoders (VAEs) [7], generative adversarial networks (GANs) [8], diffusion models [9], and long short-term memory (LSTM) networks [10], are good at capturing nonlinear temporal relationships and producing high-dimensional synthetic data. Nevertheless, they tend to have poor interpretability, demand extensive training data, and perform poorly in generalizing to rare, high-impact events like typhoons. Conversely, probabilistic approaches, such as Markov chains [11], Gaussian processes [12], time series models [13], and copula functions [14], provide more transparent uncertainty quantification and greater robustness. However,

existing studies have failed to fully describe the spatiotemporal complexity and nonlinear interactions of power systems under extreme weather conditions. Furthermore, it fails to reflect the compound risks of renewable output variability and grid faults induced by typhoon dynamics [15].

To address these limitations, this study proposes an intelligent scenario generation framework tailored for weekly. The proposed method improves the accuracy of the scenarios by capturing the spatio-temporal impacts of typhoons on renewable energy power generation, load demand and transmission infrastructure, and supports risk-aware resilient planning. The key contributions of this study are:

(1) Developing a hybrid scenario generation approach that combines ARIMA-based deterministic forecasting with Monte Carlo simulation to model the temporal trends and stochastic variations in renewable generation and load.
(2) Constructing a numerical integration-based model to estimate line fault probabilities as a function of typhoon wind intensity for quantitative operational risk assessment.
(3) Proposing a clustering-based scenario selection strategy to extract representative and extreme source–grid–load trajectories under typhoon conditions on both daily and weekly timescales.
(4) Establishing a multi-scenario dynamic simulation framework to evaluate system operational stability and aid in optimized dispatch, fault prevention strategies, and resilience assessments.

2. Scenario Generation Models for Typhoon-Driven Power System Operations

2.1. Framework Overview

Typhoons, as extreme weather events, greatly increase uncertainties in power system operations due to complex temporal fluctuations, nonlinear source-grid-load coupling, and random fault risks. Consequently, this study develops a dedicated layered scenario generation framework for weekly and daily power system operations under typhoon conditions to capture these multidimensional uncertainties and facilitate dispatch optimization.

As illustrated in Figure 1, the proposed framework consists of the following key modules:

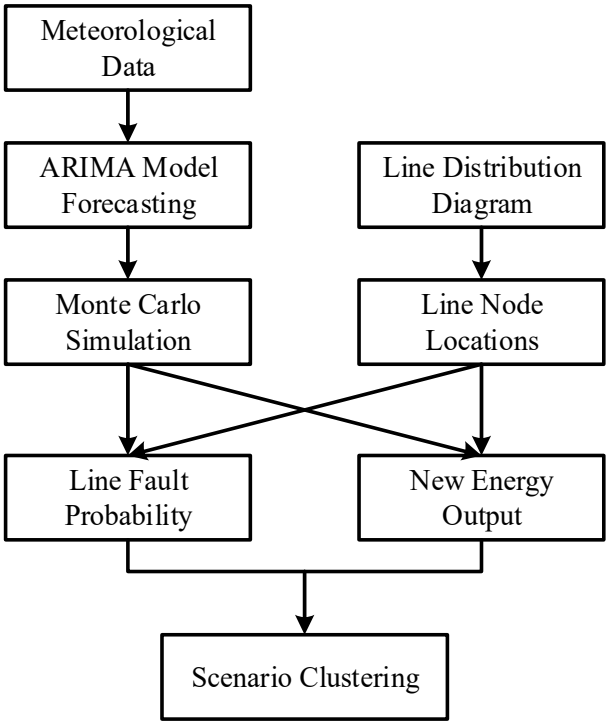

Figure 1. Typhoon-Condition Power System Scenario Framework.

This framework integrates four core modules to capture multidimensional uncertainties in power system operations under typhoons: ARIMA-based deterministic forecasting for wind speed and load trends, Monte Carlo simulation for stochastic scenario generation, numerical integration-based line fault probability modeling, and spectral clustering-K-means for extracting representative and extreme scenarios. The interaction between modules is as follows:

(1) The ARIMA model first generates deterministic time-series baselines for wind speed and load by learning historical typhoon data, capturing trends such as sustained wind speed increases along typhoon trajectories. These baselines serve as the foundational input for subsequent stochastic modeling.
(2) The Monte Carlo simulation module takes the ARIMA-generated baselines as reference, introducing random noise terms to perturb the deterministic trajectories. This process expands the single baseline into an ensemble of stochastic scenarios, quantifying uncertainties in renewable output and load caused by typhoon-induced gusts or prediction errors.
(3) The fault probability model uses wind speed outputs from both ARIMA baselines and Monte Carlo scenarios to calculate transmission line fault risks via vulnerability curves. Specifically, it maps wind speed values to fault probabilities, linking meteorological uncertainties to grid infrastructure risks.
(4) Finally, the stochastic source-load profiles and line fault probabilities are integrated into a unified scenario space, which is then processed by the clustering module to extract representative and extreme scenarios for system stability evaluation.

This integrated workflow realizes the end-to-end conversion from raw typhoon meteorological data to a scenario library, reflecting both deterministic and stochastic characteristics of system operation under typhoon disturbances.

2.2. Forecasting with ARIMA for Typhoon-Induced Wind Speed Characteristics

Under typhoon conditions, the temporal evolution of renewable energy generation and load demand demonstrates distinct deterministic patterns, such as sustained wind speed increases along typhoon trajectories. These patterns necessitate the construction of a deterministic forecasting baseline via the ARIMA model [16]. Based on historical wind power and load time series under typhoon scenarios, the Augmented Dickey-Fuller (ADF) test is applied to assess stationarity, and the differencing order is selected to eliminate non-stationary trends. Autocorrelation Function (ACF) and Partial Autocorrelation Function (PACF) analyses are subsequently performed to determine the autoregressive order p and moving average orders q. The model parameters are optimized via Maximum Likelihood Estimation (MLE), and the ARIMA model is mathematically formulated as:

$$\left(1-\sum_{i=1}^{p}\phi_i L^i\right)(1-L)^d y_t = \left(1+\sum_{j=1}^{q}\theta_j L^j\right)\epsilon_t \tag{1}$$

where L denotes the lag operator, and $\epsilon_t \sim N(0,\sigma^2)$ represents the Gaussian white noise term. After model training, the Ljung-Box test is conducted to validate the whiteness of residuals, thereby confirming that temporal correlations have been adequately captured. The deterministic forecasts $\hat{y}_t$ generated by ARIMA effectively capture the temporal evolution of wind power and load under typhoon conditions, such as sustained high-intensity wind speed fluctuations along typhoon trajectories. These deterministic sequences provide a baseline temporal framework for the subsequent Monte Carlo-based stochastic scenario generation, ensuring that simulated trajectories remain consistent with the physical evolution of typhoon-induced meteorological processes.

2.3. Typhoon-Driven Line Fault Probability Modeling Based on Wind Stress and Numerical Integration

2.3.1. Wind Speed Probability and Line Fault Modeling in Typhoon Scenarios

Due to the uncertainty in typhoon trajectories and wind speed distribution, typhoons introduce complex uncertainties into power system operations. To accurately characterize the spatiotemporal features of wind speed during typhoon events, a path-based wind speed and transmission line fault probability model is established, as illustrated in Figure 2.

The above figure depicts the spatial distribution of wind speed at different geographical locations relative to the typhoon center, with wind speed determined by parameters like distance from the typhoon center, radius of maximum wind speed, and correction coefficient, which is crucial for modeling transmission line fault probabilities induced by typhoon wind stress.

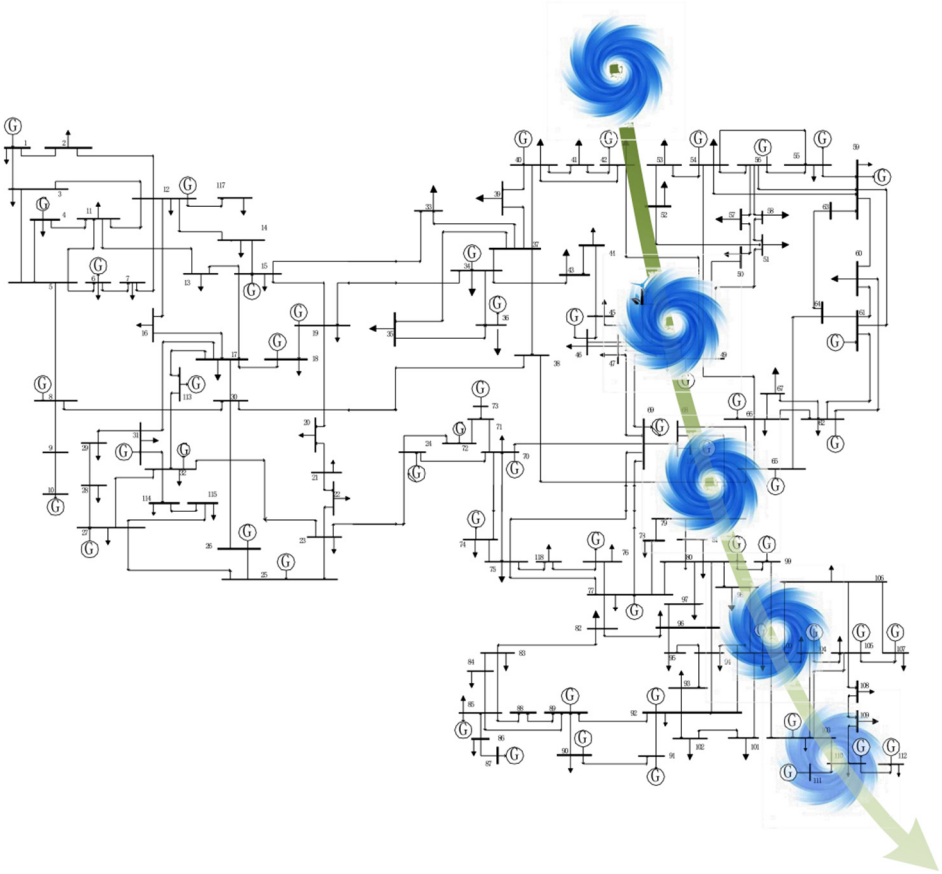

Figure 2. Schematic representation of the typhoon trajectory.

(1) Modeling of Wind Speed Induced by Typhoons:

Multiple possible typhoon trajectories are delineated from historical typhoon records, with each trajectory assigned a probability based on meteorological statistical analysis. The relationship between typhoon trajectories and corresponding wind speeds is expressed as follows:

$$V = \begin{cases} K_V \left(\dfrac{r}{R_{\max}} \right)^{T_{typ}} V_{\max} & r \in [0, R_{\max}) \\ K_V \left(\dfrac{R_{\max}}{r} \right)^{T_{typ}} V_{\max} & r \in [R_{\max}, \infty) \end{cases} \tag{2}$$

where V represents the wind speed at various geographical locations within the corresponding region, T_{typ} is a tuning parameter for adjusting the wind speed distribution, K_V is a correction coefficient, r represents the distance from the region to the typhoon center, R_{max} is the radius of maximum wind speed, and V_{max}indicates the typhoon's maximum wind speed.

(2) Spatiotemporal Quantification of Wind Speed Prediction Error:

The spatiotemporal characteristics of wind speed prediction errors during typhoon events are quantified by integrating ARIMA forecasting with Monte Carlo perturbation methods. Temporally, the prediction error progressively increases throughout the typhoon's lifecycle, ranging from approximately ±1 m/s in the initial phase to ±3 m/s during the mature phase. Spatially, the distribution of prediction errors across measurement nodes varies according to the specific typhoon trajectory. For example, under Trajectory 1, coastal nodes experience a wind speed error standard deviation of up to 1.2 m/s, whereas inland nodes along Trajectory 3 display a lower standard deviation of approximately 0.8 m/s, indicating terrain's modulating influence on error propagation.

$$v_t^{(k)} = \hat{v}_t + \epsilon_t^{(k)}, \epsilon_t^{(k)} \sim N(0, \sigma_t^2) \tag{3}$$

where $\hat{v}_t$ represents the wind speed forecasted by the ARIMA model, and σ_t^2 denotes the time-dependent variance matrix that characterizes the spatial heterogeneity of prediction errors.

2.3.2. Wind Speed and Power System Scenario Model

The wind turbine power output is generated based on the wind speeds under typhoon conditions. The operational characteristics of a wind turbine are typically defined by three critical parameters: cut-in wind speed V_{in}, rated wind speed V_r, and cut-out wind speed V_{out}. These parameters determine the shape of the turbine's power output curve, which is derived from the physical principles of wind energy conversion—including the influence of air density, turbine swept area, and conversion efficiency on energy capture. To simplify the modeling process, this study assumes uniform wind speed and direction across all turbines within a given wind area—a simplification that explicitly ignores spatial variability caused by terrain differences, turbine wake effects, and local wind turbulence. While this assumption may slightly underestimate actual output fluctuations (as real-world wind conditions vary across different turbine locations), it allows the entire wind area to be represented by an equivalent single turbine, balancing model complexity with computational feasibility. Its power output is described by the following piecewise function:

$$P_w = \begin{cases} 0 & 0 \le V \le V_{in} \\ (A + BV + CV^2)P_r & V_{in} \le V \le V_r \\ P_r & V_r \le V \le V_{out} \\ 0 & V \ge V_{out} \end{cases} \tag{4}$$

where P_r represents the rated power of the wind turbine. The above function encapsulates the relationship between wind speed and power output, integrating the aforementioned physical principles into its piecewise structure. The constants *A*, *B*, and *C* are calculated as follows:

$$A = \frac{V_{in}(V_{in} + V_r) - 4(V_{in}V_r)\left(\frac{V_{in} + V_r}{2V_r}\right)^3}{(V_{in} - V_r)^2} \tag{5}$$

$$B = \frac{4(V_{in} + V_r)\left(\frac{V_{in} + V_r}{2V_r}\right)^3 - (3V_{in} + V_r)}{(V_{in} - V_r)^2} \tag{6}$$

$$C = \frac{2 - 4\left(\frac{V_{in} + V_r}{2v_r}\right)^3}{(V_{in} - V_r)^2} \tag{7}$$

where the parameters are set as follows: $V_{in} = 3$ m/s, $V_r = 25$ m/s, $V_{out} = 35$ m/s, $p_r = 80$ MW.

In addition to affecting wind power generation, typhoon-induced winds significantly increase the risk of transmission line failures. Therefore, this study introduces a probabilistic model to quantify transmission line failure under typhoon-induced wind stress. The model explicitly accounts for transmission line faults in the receiving-end power system caused by typhoon conditions. The relationship between line failure probability and typhoon wind speed is characterized using a wind vulnerability curve, defined as follows:

$$p_f = \begin{cases} 0 & V \le v \\ exp\left(\frac{\beta(V - v)}{v}\right) - 1 & v < V \le 2v \\ 1 & V > 2v \end{cases} \tag{8}$$

where p_f represents the probability of line failure,v is the maximum wind resistance speed of the transmission line, and β is the coefficient of the vulnerability curve. Here, v is determined based on the structural attributes of the transmission lines examined in this study, marking the wind speed threshold above which the risk of line failure begins to manifest; β functions as a parameter to modulate how responsive the fault probability is to wind speeds exceeding v, aligned with the scenario generation framework to capture the nonlinear association between wind intensity and the likelihood of failure.

$$p_0(Z_n) = \frac{\sum_{i=1}^{I(n)} p_{f,i}}{\sum_{n=1}^{N}\sum_{i=1}^{I(n)} p_{f,i}} \tag{9}$$

where $I(n)$ represents the set of failed transmission lines under fault scenario Z_n, and N denotes the set of all fault scenarios.

2.4. Monte Carlo Simulation for Stochastic Scenario Ensemble Generation

While ARIMA-based deterministic forecasting can capture temporal trends, it cannot quantify meteorological forecast errors or the stochastic variations in renewable energy generation. To address this, the Monte Carlo simulation is combined with the ARIMA baseline model to produce a set of stochastic scenarios that represent uncertainties associated with extreme typhoon weather conditions. Specifically, the white noise variance σ^2 is estimated from historical residuals to derive random noise terms $\epsilon_t^{(k)}$ that satisfy condition $N(0, \sigma^2)$. These noise terms are subsequently superimposed onto the ARIMA-predicted values to obtain stochastic scenario realizations, expressed as:

$$y_t^{(k)} = \hat{y}_t + \epsilon_t^{(k)}, \quad k = 1,2, \ldots, N \tag{10}$$

This process simulates stochastic phenomena including typhoon-induced gust intensity fluctuations and generates diversified scenarios through noise perturbation. The Monte Carlo method augments ARIMA-based deterministic forecasts by generating statistically representative ensembles of stochastic scenarios, which serve as essential inputs for subsequent transmission line fault probability estimation and clustering analysis.

2.5. Scenario Clustering and Reduction via Probabilistic Feature Metrics

The hybrid framework proposed combines spectral clustering and K-means. It first uses kernel-based spectral mapping for nonlinear dimensionality reduction, then extracts centroids to identify representative typhoon-induced risk scenarios. The selection of this hybrid approach is motivated by the unique characteristics of typhoon-induced power system scenarios, offering distinct advantages over alternative methods such as probabilistic distance-based approaches:

(1) Handling nonlinearity: Typhoon scenarios involve strong nonlinear spatiotemporal correlations (e.g., interactions between wind speed fluctuations, load variations, and line fault risks). Spectral clustering via kernel functions effectively captures these nonlinear relationships, whereas probabilistic distance-based methods (relying on linear metrics) often fail to model such complexities.

(2) Preserving extreme features: Extreme scenarios (e.g., peak wind speeds or severe fault risks) critical for resilience assessment are retained through spectral clustering's dimensionality reduction, while K-means ensures their distinctiveness. Probabilistic distance-based methods may smooth out these extreme features due to averaging effects.

(3) Computational efficiency: For high-dimensional scenario sets integrating wind speed, load, and fault probabilities, spectral clustering reduces dimensionality to lower computational complexity, and K-means efficiently clusters the reduced features—outperforming probabilistic distance-based methods that struggle with scalability in high-dimensional spaces.

This preserves key features of extreme typhoon scenarios and reduces the complexity of scenario set representation, thus improving the efficiency of scenario-based modeling in storm-resilient power system planning.

Initially, wind power scenarios associated with typhoon conditions are standardized using the Z-score method to remove dimensional inconsistencies, as expressed by the following formula:

$$x_j^{(i)} = (x_j^{(i)} - \mu_j)/\sigma_j \tag{11}$$

where μ_j and σ_j represent the mean and standard deviation of the jth dimensional feature, respectively. Subsequently, a Gaussian kernel function is utilized to construct the similarity matrix among wind power scenarios under typhoon conditions:

$$W_{i,j} = exp\left(-\frac{\|x^{(i)} - x^{(j)}\|^2}{2\sigma^2}\right) \ (i \neq j) \tag{12}$$

The kernel parameter σ is optimized through grid search to adaptively capture localized correlation features among wind speed, wind power output, and fault-prone nodes under typhoon conditions. The Gaussian kernel function enhances the similarity weights among neighboring typhoon scenarios through its exponential decay property, thereby suppressing irrelevant disturbances. Compared to the Euclidean distance metric, it exhibits

superior capability in capturing the spatial synchronicity and temporal continuity of wind power fluctuations under typhoon-induced conditions.

Building upon this foundation, a normalized Laplacian matrix is constructed in accordance with graph signal processing theory:

$$L_{\text{sym}} = I - D^{-1/2} W D^{-1/2} \tag{13}$$

where the diagonal elements of the degree matrix D correspond to the row-wise summation of the similarity matrix.

The Laplacian matrix L_{sym} is decomposed into its eigencomponents, and the eigenvectors corresponding to the k smallest eigenvalues are selected to project the original high-dimensional wind power scenarios onto a low-dimensional manifold space. This procedure leverages the spectral characteristics of the Laplacian matrix to uncover the intrinsic manifold structure of typhoon-related data, enabling the mapping of complex causal chains—such as rapid power fluctuations induced by intense wind activity, transmission line stress, and cascading relay protection responses—into a latent feature space while effectively reducing redundant dimensional components.

To enhance the robustness of clustering under typhoon-induced wind power scenarios, the low-dimensional feature matrix is subjected to row-wise L2 normalization, thereby mitigating the impact of vector magnitude differences on similarity measurements. Subsequently, the K-means algorithm is applied to minimize the within-cluster sum of squared distances, thereby identifying representative scenario prototypes associated with typical typhoon conditions.

$$J = \sum_{c=1}^{k} \sum_{V_i \in C_c} \|V_i - \mu_c\|^2 \tag{14}$$

The optimal number of clusters k is determined by locating the elbow point on the Sum of Squared Errors (SSE) curve, which reflects the balance between clustering accuracy and model complexity. In addition, silhouette coefficients are utilized to quantitatively evaluate inter-cluster separability. Focusing on typhoon-induced scenarios, once the iterative clustering process converges, typical scenario patterns are identified, with each cluster centroid encapsulating the statistical characteristics of representative typhoon events, thereby enabling structured scenario generation for subsequent analysis.

The cluster centroids derived from the clustering process can be directly employed to support pre-simulation analysis of power system dispatch strategies. Specifically, for high wind speed patterns characteristic of typhoon scenarios, the reserve capacity optimization model is formulated as follows:

$$P_{\text{extra}} = max(\mu_c + 3\sigma_c, P_{\text{baseline}}) \tag{15}$$

Furthermore, real-time disaster data under typhoon conditions can be incorporated into the clustering model to facilitate online adaptation of the Gaussian kernel parameter σ and recalibration of the feature vector dimensionality k, thereby establishing a closed-loop learning framework that integrates scenario generation, clustering-based dimensionality reduction, strategy optimization, and data-driven feedback.

2.6. Extreme Scenario Generation under Typhoon Conditions

To assess the impact of wind power shortfalls on grid security under typhoon conditions, extreme scenarios are generated based on the evaluation of clustered representative scenarios, with the objective of identifying system vulnerabilities and optimizing dispatch strategies. Based on these clustered representative typhoon scenarios, the key risk metric, Power Deficit (PD), is defined as follows:

$$PD = \sum_{t=1}^{T} \max\left(0, L_t - P_t^{\text{wind}} - P_t^{\text{backup}}\right) \tag{16}$$

where L_t denotes the load demand at time t, P_t^{wind} represents the wind power output, and P_t^{backup} denotes the backup power capacity. The scenario exhibiting the highest Power Deficit value within the clustered typhoon scenarios is identified as the worst-case scenario, reflecting the maximum risk threshold encountered by the system under typhoon conditions.

3. Evaluation of Typhoon-Induced Power System Operation Scenarios on Daily and Weekly Timescales

3.1. Overview of Simulation Setup and Test System

Typhoon path and wind speed data are obtained from the China Meteorological Administration's Best Track Dataset for Tropical Cyclones, with a temporal resolution of one hour. The simulation is based on the IEEE 118-bus system, with wind resistance design parameters for transmission lines referenced from the Design Specifications for Wind-Resistant Power Systems.

All scenario generation processes were executed using Matlab 2022b and PyCharm 2020.1.1 on a system equipped with an Intel Core i5-12400 CPU (2.50 GHz) and 16 GB RAM.

3.2. Daily-Scale Scenario Simulation and Evaluation

To assess the proposed daily scenario generation method's performance, simulations are run under typical typhoon transit conditions. Using ARIMA-based wind speed and load forecasts during typhoons, 100 stochastic scenarios are generated by adding Monte Carlo perturbations to deterministic trajectories. Then, spectral clustering with K-means extracts representative and extreme source-load scenarios, effectively capturing typhoon-induced uncertainties and spatiotemporal variations.

The following analysis focuses on three aspects: typical daily load profiles under typhoon conditions, fluctuation characteristics of normalized load and wind scenarios, and comparison between typhoon-affected and regular load curves.

As illustrated in Figure 3, under the influence of typhoon weather, three representative daily load curves show clear temporal fluctuations, with values ranging from 1.5×10^4 to 3.5×10^4. This range reflects randomness and autocorrelation in typhoon-driven demand, linked to increased use of cooling systems and emergency equipment. Though patterns vary, all curves rise gradually during daytime and peak steadily, mirroring electricity usage habits under typhoon conditions. These dynamics aid short-term forecasting and operational tweaks, like aligning reserves with daytime growth, during typhoon disturbances.

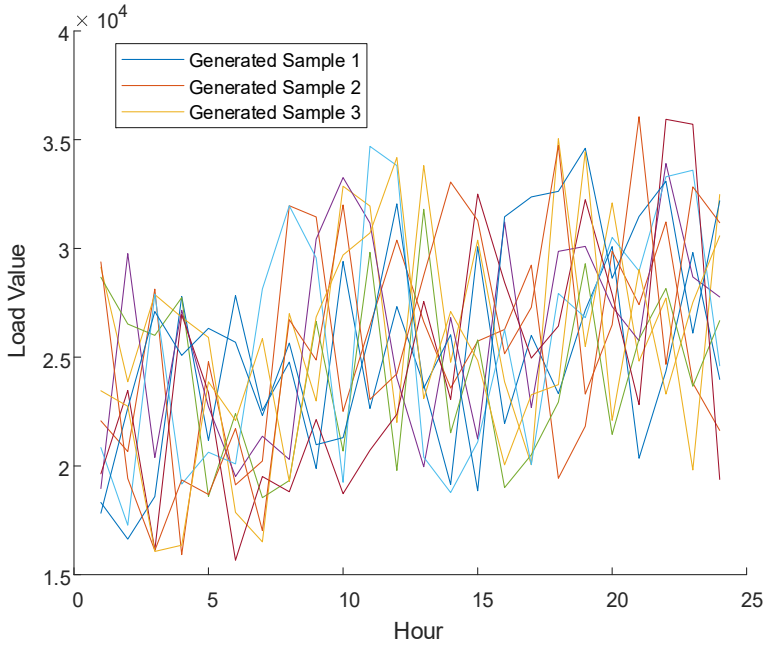

Figure 3. Daily load simulation results under typhoon conditions.

Figure 4 further depicts the normalized fluctuation characteristics of clustered daily load profiles derived from multiple stochastic scenarios. Most load values remain within the range of -2 to 2 after normalization, suggesting that although load uncertainty exists, its envelope remains physically constrained. The quasi-periodic oscillations observed across all profiles reflect both the volatility and regularity of load evolution under typhoon transit, further emphasizing the importance of probabilistic modeling in dispatch planning.

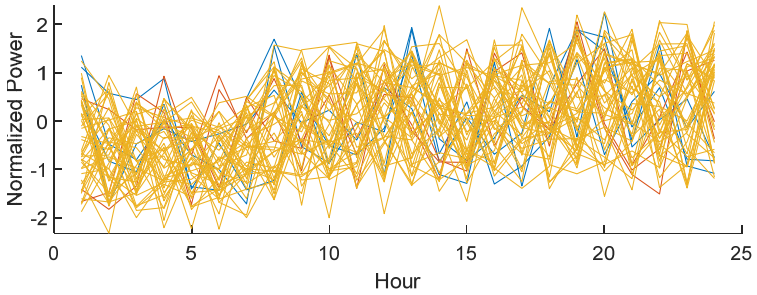

Figure 4. Normalized clustered load fluctuation profiles during typhoon transit.

To highlight the deviation of typhoon-driven load behavior from regular conditions, Figure 5 compares daily load profiles under typhoon and baseline scenarios. During the typhoon day, load increases gradually from early morning, followed by a pronounced surge in the afternoon and evening due to increased demand. Notably, the 8th-hour load reaches 30,128.71 kWh, which significantly exceeds the corresponding value under regular conditions. Despite subsequent fluctuations, the load remains elevated throughout the day. This comparison underscores the operational challenges posed by typhoon-induced demand variability and reinforces the necessity of integrating weather-driven scenarios into power system scheduling models.

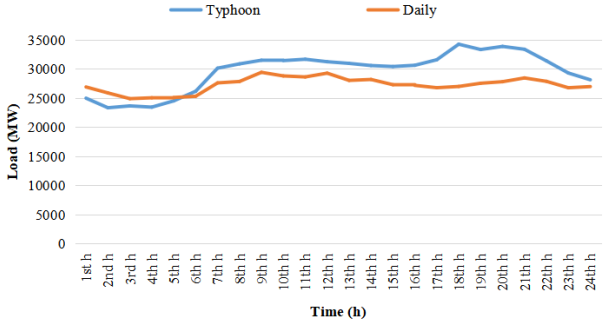

Figure 5. Comparison of daily load profiles under typhoon and regular conditions.

These daily-scale simulation results highlight the variability of load profiles under typhoon conditions and form the basis for extended weekly-scale impact analysis presented in the next section.

Building upon the daily-scale results, the following section extends the analysis to the weekly timescale to capture longer-term variability introduced by typhoon events.

3.3. Weekly-Scale Scenario Simulation and Evaluation

To extend the analysis to the weekly timescale, this section examines the spatiotemporal features of wind power and load scenarios under typhoon conditions, focusing on three aspects: sampled wind power trajectories, clustered representative curves, and typical weekly load patterns.

At the weekly level, wind power output under typhoon conditions exhibits significant volatility. As shown in Figure 6, a distinct generation peak occurs between the 80th and 87th hours, corresponding to the period of direct typhoon impact. This surge in output results from intensified wind speeds driving a transient aerodynamic response from wind turbines.

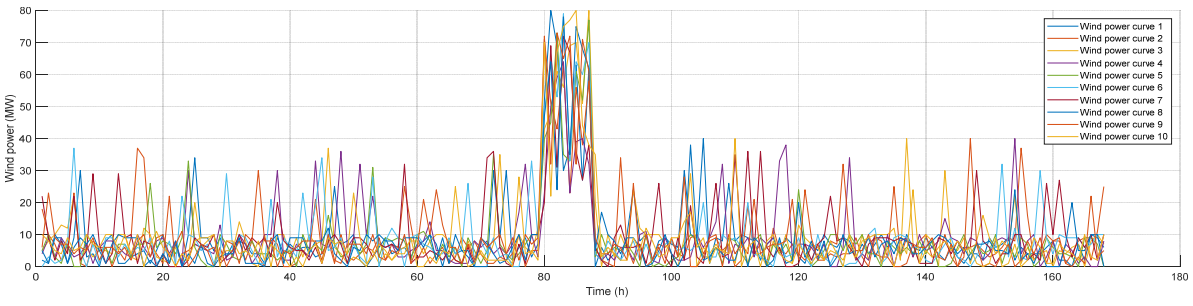

Figure 6. Sampled weekly wind power trajectory under typhoon conditions.

Figure 7 presents multiple simulated wind power trajectories during the typhoon passage, vividly capturing the dynamic response of wind generation to extreme wind conditions. Most profiles exhibit elevated power output concentrated between the 80th and 87th hours—the period of closest typhoon approach—with peak values reaching approximately 80 MW, directly reflecting the intensification of wind energy capture under high wind speeds. The varying amplitude and duration of this surge across trajectories stem from typhoon-specific factors: stronger typhoon intensity amplifies peak output, while a more direct trajectory relative to wind installations prolongs the high-output window, and geographical distance from the storm center modulates overall intensity. This variability contrasts sharply with the stable output under normal conditions, emphasizing the need for scenario-based modeling to account for typhoon-driven fluctuations—a critical step in enhancing the adaptability of dispatch strategies to extreme weather-induced generation uncertainty.

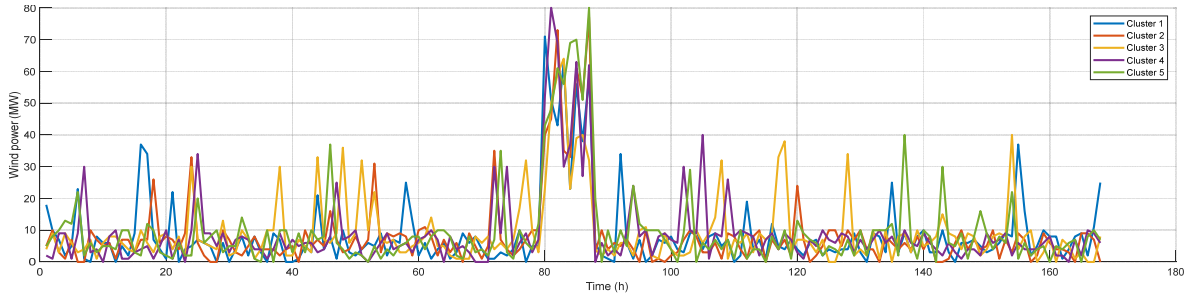

Figure 7. Clustered representative weekly wind power profiles during typhoon transit.

In parallel, weekly load dynamics also show marked responses to typhoon events. As illustrated in Figure 8, the simulated weekly load trajectory reveals a steadily rising trend throughout the event. Load increases from 633,118.80 kWh on Day 1 to 764,896.18 kWh on Day 6, followed by a slight decrease to 742,779.14 kWh on Day 7. Despite this decline, the overall load remains elevated. Compared to baseline conditions, the load profile during typhoons shows more pronounced temporal variation, likely driven by increased electricity usage and adaptive operational behaviors in residential and commercial sectors.

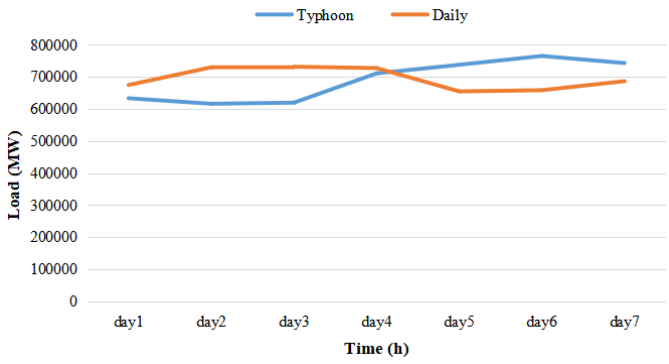

Figure 8. Comparison of weekly load profiles under typhoon and regular conditions.

This integrated analysis of wind power and load variations under typhoon conditions provides a comprehensive understanding of their joint uncertainty at the weekly scale. The insights derived support the development of robust scheduling strategies and resilience-oriented planning frameworks for typhoon-prone power systems.

This integrated analysis of wind power and load variations under typhoon conditions provides a comprehensive understanding of their joint uncertainty at the weekly scale. The insights derived support the development of robust scheduling strategies and resilience-oriented planning frameworks for typhoon-prone power systems.

This joint variation in wind generation and load at the weekly scale underscores the operational complexity introduced by typhoon events, necessitating integrated dispatch strategies.

In addition to source-load dynamics, typhoons also increase the likelihood of physical failures within the grid infrastructure. This motivates the analysis of transmission line fault probabilities under wind-induced stress conditions.

3.4. Grid Fault Probability and Load-Power Imbalance Analysis

Typhoons pose a significant threat to power system infrastructure, particularly to overhead transmission lines. This section examines the increased probability of line faults during typhoon events and its impact on grid stability. As shown in Figure 9, the probability of transmission line faults exhibits a pronounced upward trend during typhoon events. The likelihood of transmission line failures rises sharply, particularly during peak typhoon wind speeds, resulting in elevated fault exposure across coastal and path-adjacent corridors. This heightened risk of line outages is particularly evident in coastal areas or along the typhoon's path, where lines experience more severe wind stress compared to inland regions. The spatial variation in fault probability underscores the importance of considering geographical factors when assessing grid vulnerability under typhoon conditions. This analysis highlights the critical need to incorporate weather-driven fault probability assessments into power system modeling, enabling grid operators to better anticipate and mitigate the impacts of extreme weather events on transmission infrastructure. Incorporating this spatially resolved fault probability into dispatch planning helps enhance preventive control and fault-tolerant capability of the grid.

To translate these findings into system-level planning insights, a resilience-oriented assessment is conducted, focusing on extreme scenarios extracted from the probabilistic ensemble.

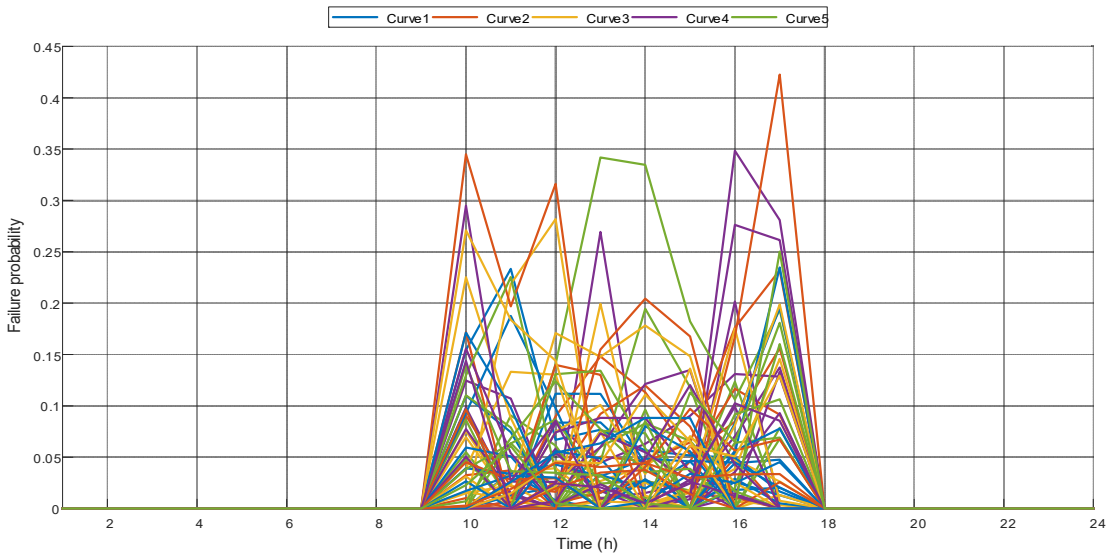

Figure 9. The fault probability curve for each transmission line.

3.5. System Resilience Assessment under Typical and Extreme Scenarios

To further evaluate operational resilience, this section analyzes system behavior under typical and worst-case typhoon scenarios from scenario clustering. It assesses dispatch stress by examining daily and weekly worst-case net load conditions. Assessing system resilience from supply and demand sides is crucial for stable power system operation during extreme weather. This section evaluates the system's ability to maintain operational balance under typhoon scenarios, focusing on net load dynamics influenced by renewable generation fluctuations and demand pattern shifts.

As shown in Figures 10 and 11, under the influence of a typhoon, both the daily and weekly load demands exhibit relatively stable trends, while the output from renewable energy sources nearly drops to zero, causing the net load to closely match the load demand. These results indicate that renewable generation capacity is severely diminished during typhoons, increasing reliance on traditional energy sources, while also making power dispatch more complex.

At the weekly time scale, the volatility of the net load is even more pronounced under the typhoon scenario, particularly around the typhoon's landfall when the net load reaches peak values. This short-lived but intense impact highlights the need for the grid to have sufficient flexibility and reserve capacity to cope with the uncertainty in wind power generation and the increased load demand.

These results demonstrate that typhoons significantly reduce the availability of renewable energy, leading to higher and more volatile net load levels. This analysis underscores the necessity of enhancing grid flexibility through reserve capacity, demand-side management, and energy storage systems to improve system resilience against extreme weather-induced disturbances.

This resilience assessment validates the necessity of weather-informed scenario planning and provides a quantitative basis for enhancing grid robustness under future typhoon events.

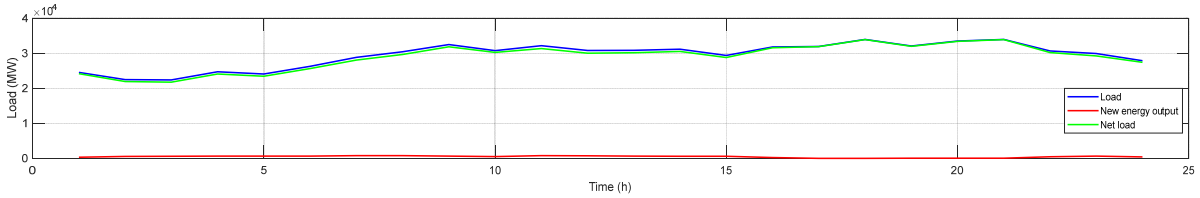

Figure 10. The worst-case load scenario at the daily scale under typhoon conditions.

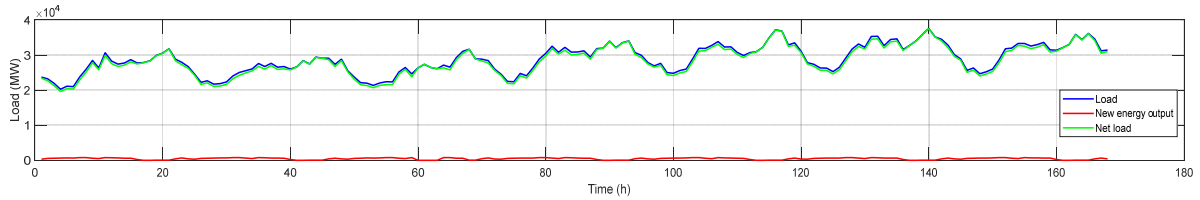

Figure 11. The worst-case load scenario at the weekly scale under typhoon conditions.

4. Conclusions and Future Work

This study proposes an intelligent uncertainty scenario generation framework tailored to power system operations under typhoon-induced extreme weather conditions at both daily and weekly timescales. By integrating ARIMA-based deterministic forecasting with Monte Carlo-driven stochastic perturbations, capture complex uncertainties. A numerical integration-based fault probability model is developed to quantitatively assess the wind-induced risk of transmission line outages, while a combination of spectral clustering and K-means is employed to extract representative and extreme source–load joint scenarios from high-dimensional ensembles. Herein, the clustering process is explicitly positioned as a preliminary assessment step with its core output being an extreme scenario set that constitutes the focus of this study. This set retains critical features of high-impact typhoon events such as extreme wind speeds severe line faults and load-generation imbalances while balancing computational feasibility ensuring it serves as a robust foundation for subsequent analyses.

Overall, this work presents a unified and data-informed modeling framework for dispatch optimization, fault risk assessment, and resilience enhancement under typhoon conditions. The proposed method accurately captures the spatiotemporal uncertainties introduced by typhoons and reveals their compound impacts on renewable energy intermittency, load volatility, and transmission reliability.

Notably, the extreme scenario set generated in this study is designed to support follow-up research where targeted evaluations such as detailed stability analysis scenario-specific resilience quantification and refined dispatch strategy optimization will be conducted. This phased approach ensures that the preliminary clustering in this work does not permanently eliminate potential extreme scenarios but rather focuses on identifying a manageable yet informative subset with subsequent studies enabling in-depth exploration of extreme cases including potential re-examination of the original scenario pool to ensure comprehensive coverage of high-impact events.

Future research could extend this framework to encompass other categories of extreme weather—such as heavy snow, heatwaves, or compound events—and incorporate advanced generative models or adaptive clustering techniques to further improve the realism and computational efficiency of scenario generation and reduction.

Author Contributions

J.W.: conceptualization, methodology, supervision, project administration, writing—reviewing and editing; M.L.: software, formal analysis, data curation, visualization, writing—original draft preparation; N.Y.: methodology, validation, writing—reviewing and editing; Z.S.: investigation, software support; J.C.: data collection, resources; Y.Z.: visualization support; X.H.: funding acquisition, project coordination. All authors have read and agreed to the published version of the manuscript.

Funding

This research received no external funding.

Institutional Review Board Statement

Not applicable.

Informed Consent Statement

Not applicable.

Data Availability Statement

The simulation data contain confidential information and are not publicly disclosed. A summary of the results is presented within the manuscript, and the simulation framework is elaborated in the Methods section. For data access requests, please contact the corresponding author via email.

Conflicts of Interest

The authors declare no conflict of interest.

References

1. The Central People's Government of the People's Republic of China. Xi Jinping Presided over the 9th Meeting of the Central Financial and Economic Affairs Commission. 2024. Available online: http://www.gov.cn/xinwen/2021-03/15/content_5593154.htm (accessed on 15 May 2025).
2. Yang, Y.; Sun, Y.-Y.; Mao, Z.-H.; et al. Generation Method for Extreme Wind Power Scenarios Induced by Mid-term Weather Processes. *Proc. CSEE* **2024**, *1*, 1–11.
3. World Meteorological Organization. State of the Global Climate 2023. WMO, 2024. Available online: https://wmo.int/publication-series/state-of-global-climate-2023 (accessed on 19 May 2025).
4. Gao, Z.-T.; Zhang, J.; Li, Y.; et al. Impact of Extreme Weather on Local Wind Conditions in Wind Farms. *J. Huazhong Univ. Sci. Technol.* **2024**, *52*, 106–112.
5. Yang, N.; Xu, G.; Fei, Z.; et al. Two-Stage Coordinated Robust Planning of Multi-Energy Ship Microgrids Considering Thermal Inertia and Ship Navigation. *IEEE Trans. Smart Grid* **2025**, *16*, 1100–1111. https://doi.org/10.1109/TSG.2024.3524550.
6. Dong, X.-C.; Zhang, S.; Li, Y.; et al. Review of Sequential Scenario Generation and Reduction Methods in Power Systems. *Power Syst. Technol.* **2023**, *47*, 709–721.
7. Wang, X.-Y.; Li, Y.; Dong, X.-C.; et al. Multi-source and Load Scenario Generation Method for Active Distribution Networks Based on Variational Autoencoder. *Power Syst. Technol.* **2021**, *45*, 2962–2969.
8. Kang, M.Y.; Zhu, R.; Chen, D.X.; et al. A Cross-modal Generative Adversarial Network for Scenarios Generation of Renewable Energy. *IEEE Trans. Power Syst.* **2024**, *39*, 2630–2640.
9. Dong, X.-C.; Mao, Z.-H.; Sun, Y.-Y.; et al. Short-term Wind Power Scenario Generation Based on Conditional Latent Diffusion Models. *IEEE Trans. Sustain. Energy* **2024**, *15*, 1074–1085.
10. Wang, J.; Yu, J.; Kong, X. Mid- to Long-term Load Forecasting Model Based on Dual Decomposition and Bidirectional Long Short-term Memory Network. *Power Syst. Technol.* **2024**, *48*, 3418–3426.
11. Munkhammar, J.; van der Meer, D.; Widén, J. Very Short Term Load Forecasting of Residential Electricity Consumption Using the Markov-chain Mixture Distribution (MCM) Model. *Appl. Energy* **2021**, *282*, 116180.
12. Sharifzadeh, M.; Sikinioti-Lock, A.; Shah, N. Machine-learning Methods for Integrated Renewable Power Generation: A Comparative Study of Artificial Neural Networks, Support Vector Regression, and Gaussian Process Regression. *Renew. Sustain. Energy Rev.* **2019**, *108*, 513–538.
13. Lucheroni, C.; Boland, J.; Ragno, C. Scenario Generation and Probabilistic Forecasting Analysis of Spatio-temporal Wind Speed Series with Multivariate Autoregressive Volatility Models. *Appl. Energy* **2019**, *239*, 1226–1241.
14. Zhou, N.; Xu, X.; Yan, Z.; et al. Spatio-temporal Probabilistic Forecasting of Photovoltaic Power Based on Monotone Broad Learning System and Copula Theory. *IEEE Trans. Sustain. Energy* **2022**, *13*, 1874–1885.
15. Yang, N.; Xiong, Z.; Ding, L.; et al. A Game-based Power System Planning Approach Considering Real Options and Coordination of All Types of Participants. *Energy* **2024**, *312*, 133400. https://doi.org/10.1016/j.energy.2024.133400.
16. Ye, L.; Pei, M.; Yang, J.-B.; et al. Power Balance Mechanism in New Energy Power Systems Under Extreme Weather Conditions. *Autom. Electr. Power Syst.* **2025**, *49*, 2–18.